AD-A047 484 MICHIGAN UNIV ANN ARBOR CAVITATION AND MULTIPHASE FL--ETC F/G 20/4
CAVITATION DAMAGE PREDICTING CAPABILITY - STATE OF ART AND POSS--ETC(U)
AUG 77 F G HAMMITT, M K DE N00014-76-C-0697

UNCLASSIFIED UMICH-014456-23-I NL

| OF |
AD
A047484

END
DATE FILMED
1 -78
DDC

UNIVERSITY OF MICHIGAN
Department of Mechanical Engineering
Cavitation and Multiphase Flow Laboratory

Report No. UMICH-014456-23-I

CAVITATION DAMAGE PREDICTING CAPABILITY - STATE OF ART AND POSSIBILITIES

(To be presented at Symposiun on Erosion: Prevention and Useful Applications, ASTM Comm. G-2 Conference, Vail, Colorado, October 24-26, 1977)

by
F. G. Hammitt
M. K. De

Supported by ONR Contract No. N00014-76-C-0697

35p.

August 15, 1977

ABSTRACT

New results from cavitating venturi water tests are used to reinforce the concept of "cavitation erosion efficiency", previously developed here from tests in a vibratory facility with both water and sodium.(8,9). This concept emerges from a technique herein described to allow a priori prediction of eventual cavitation erosion rates in flowing machines. Bubble collapse pulse height spectra obtained from submerged microprobes are correlated with measured erosion rates in given laboratory and/or field devices to allow this prediction. Preliminary results from such correlations, along with other measurements of the effects of gas content, velocity, and cavitation condition upon "mechanical" cavitation intensity as measured by the pulse height spectra, are here presented.

New results from vibratory facility tests in tap water and synthetic sea water upon three materials of variable corrodibility (304 SS, 1018 carbon steel, and 1100-0 aluminum) are also presented. The ratio between maximum erosion rates for the salt and fresh water tests are found to increase toward unity as the mechanical cavitation intensity is increased, i.e., increased MDPR. This is expected on theoretical grounds.

Finally, the relation between incubation period and maximum MDPR is examined from the vibratory test results, and found to depend upon the material properties as well as the fluid-flow conditions.

I. INTRODUCTION

One of the major difficulties facing designers of liquid-flow machinery where cavitation is a possibility, is the present almost complete inability to predict eventual cavitation damage rates, or even their probable existence, from reasonably practical laboratory tests. Hence very expensive long-term cavitation damage tests in near prototype scale conditions are often necessary. The primary purpose of the University of Michigan research here described is to provide new data and techniques from laboratory-scale work to help to bridge this gap in predicting capability.

It is hoped to attain this goal by using relatively more sophisticated acoustic techniques than have been generally applied to this problem in the past. The relationship between general cavitation noise and erosion has been recently studied in several laboratories (1-7, eg.) for the purpose of predicting eventual damage rates. While no very general success has been attained, a relatively good relationship between noise level and damage rate for specific units has been observed. We hope to improve the general utility of acoustic measurements for damage prediction by a more pertinent and sophisticated analysis of the acoustic data. Rather than using total noise amplitude, or amplitude within a fixed frequency band (1-4, eg.), we have analyzed the noise in terms of a spectrum comprising the number of pressure pulses and their individual amplitude. Our initial results used a relatively standard cavitation damage "vibratory facility" (8,9), and produced quite "good" correlations between spectral "areas" and measured damage rate (MDPR = "mean depth of penetration"), as shown in Fig. 1. We further (8,9,eg.) presented these results in terms of a "cavitation erosion efficiency" (Fig. 2), which we defined to be the ratio between measured acoustic power in the cavitation field and "erosion power". This latter term we defined to be the product of volume loss

rate and material failure energy, here considered to be "ultimate resilience". This "cavitation erosion efficiency" (Fig. 2) was found to be numerically very small, as would be intuitively expected, but also remained relatively constant over a broad range of test temperature and pressure (8,9, eg.), strengthening our belief in the probable validity of the concept. Figure 2 (8,9) is typical.

Similar instrumentation installed in flow machines would allow an à priori prediction of eventual damage rates to be encountered in such machines. Such a prediction is not otherwise possible within the present state of the art. Somewhat related preliminary results are also reported from Japan (5,6, eg.) and Russia (7).

The present article provides related preliminary results from a water venturi system, as opposed to our previous water and sodium (8,9, eg.) vibratory facility results. It also presents new vibratory results designed to separate mechanical and corrosive cavitation erosion, using tests in fresh and salt water with materials of differing degrees of corrosivity, tested over a range of mechanical "intensities". Presumably the pulse spectra measure such mechanical intensities, but are insensitive to corrosive intensities. This portion of the present work will be discussed next.

II. SALT AND FRESH WATER VIBRATORY TESTS (10)

Three materials of varying corrodibility were tested in synthetic sea water (2.4% by mass NaCl) and in Ann Arbor tap water. These were 1100-0 aluminum, 304 stainless steel, and 1018 (cold-rolled) carbon steel. The "mechanical" cavitation intensity was varied for these tests by varying either/or suppression pressure* or liquid temperature. Two and three bar suppression pressures were provided by compressed air cover gas, and liquid temperature was varied from 20 to 105°C. Peak to peak horn amplitude for these tests was 1.5 mils

*Suppression pressure = $p-p_v$ = NPSH x ρ, p_v = vapor pressure

(38 μm), and horn frequency 20 kHz in all cases. Maximum MDPR** and incubation period*** were measured for each condition. All raw data and other full test details and results are reported elsewhere (10).

Figures 3 and 4 show the relation between the maximum MDPR ratio between fresh and salt water tests, and maximum MDPR itself, for 304-SS and 1018 carbon steel, respectively. For simplicity and reproducibility, the calculated least mean square best fit lines are shown, rather than best curves. For all three materials (10) the ratio increases toward unity for increased MDPR, which indicates for these tests primarily an increased mechanical intensity. The trend was greatest for carbon steel (Fig. 4) as might be expected, and least for aluminum, with 304-SS (Fig. 3) intermediate.

Figure 5 shows the relation for these tests between incubation period and maximum MDPR for 304-SS. Again the best least mean square fit straight line is computed and shown. It would be expected on intuitive grounds plus much previous test experience, that increased $MDPR_{max}$ would correspond to reduced incubation period, both corresponding in general to increased cavitation intensity for a given material, or to weaker materials for a given intensity. However, the inverse trend is shown in Fig. 5 for 304-SS and is even more pronounced for 1100-0 aluminum (Fig. 6). The curve for carbon steel, not shown, is similar to that for 304-SS (10). However, the correlation coefficients are low so that these trends may not be meaningful.

Figure 7 combines data for all materials in terms of Incubation Period vs. $MDPR_{max}$. In general the expected overall trend of decreasing incubation period for increasing $MDPR_{max}$ is shown, but there is an unexpected intermediate minimum when results for all material are combined on the

---

**MDPR = mean depth of penetration rate based on total surface area.

***Incubation period is here defined as the intercept on the abscissa of a curve of weight loss vs. test duration of the tangent drawn from the maximum slope portion of the curve.

same plot. This is caused by the strong inverse relationship for aluminum as compared to the other materials. These results all indicate that the relationship between incubation period and $MDPR_{max}$ differs substantially according to the material tested.

III. VENTURI PRESSURE PULSES AND DAMAGE (11)

A. Apparatus and Procedures

The venturi tests were made in our High-Speed Water Loop (12), capable of throat velocity up to $\sim$ 65 m/s. Figure 8 is a schematic of this facility. While there are no valves in the loop, any desired cavitation condition and throat velocity can be attained through adjustment of pump speed and surge tank (connected to the low-pressure tank) cover gas pressure. Some degree of deaereation (to $\sim$ 30% STP) is possible through a bypass stream into a vacuum spray tank. Air content is measured by Van Slyke. Any desired "degree of cavitation" in the test venturi can be obtained by a suitable adjustment of surge tank pressure and pump speed. A cooler is installed within the downstream tank to allow some control and adjustment of liquid temperature, by balance between input pump-work and cooler heat loss.

Figure 9 shows the plexiglass venturi used for the present test series, including positions of acoustic microprobes, damage specimens, and the extent of the cavitating region for cavitation conditions I and II. The venturi had been used for previous tests of a somewhat different type, and hence the additional complicating features, which are not pertinent to the present work. As indicated in Fig. 9, the erosion sample and the two microprobes are located in the same plane, which is normal to the venturi axis at a point downstream of the throat exit. Thus, assuming axial-symmetry, the erosion specimen (located flush with the venturi diffuser wall) sees the same cavitation field as the two microprobes, which are also flush with the wall. Thus a direct

correspondence is obtained between pressure pulsations as measured by the two microprobes, and erosion and pitting, at an identical flow field location.

For cavitation condition II, the apparent end of the cavitating region is the plane of the probes and erosion specimens (1100-0 aluminum for the present tests). For cavitation condition I, the visually apparent cavitation ends 35 mm upstream of the probe position (Fig. 9). Of course some more energetic and larger bubbles no doubt penetrate further.

Figure 10 shows the pressure microprobe designed and developed here (U-M probe). It was designed for use in liquids (such as liquid sodium) at temperatures to ~600°C. Sodium high-temperature tests were in fact performed in our vibratory facility (8,9), although such temperature capabilities were not required for the present tests. However, the necessity for high temperature performance with this probe did limit its natural frequency to ~ 0.1 MHz. It was calibrated against a commercial Kistler probe, Model 601A , which also proved to have a natural frequency of about the same magnitude. Both probes were used in the present work, to investigate the degree of axial-symmetry of the cavitation field.

Ideally, the pulse height spectra for the various system conditions would be obtained via a multichannel-analyzer (MCA). However, the complexity of the actual signal (Fig. 11) makes this approach difficult. On theoretical and experimental grounds (13, eg.), it is most likely that in many cases the rise time of the pressure pulses seen by the probes is well less than 1 μs, perhaps as little as 20 nanoseconds (13). Since the period of the resonant vibration of each probe is ~10 μs, it is clear that these cannot faithfully follow the pressure pulsations generated by the collapsing bubbles. Thus a single nearby collapse will generate a probe signal rise characteristic of its own natural frequency, no doubt seriously truncating the actual pulse amplitude. In

addition, the initial impulse upon the probe will be followed by probe "ringing" as seen clearly in Fig. 11, where the simultaneous outputs of both probes are displayed, and seen to be quite similar. The small background noise in the absence of large pulses is probably primarily due to fluid turbulence and other noises of electronic origin.

It is apparent from Fig. 11 that a simple MCA counting circuit would register many collapses for each actual collapse due to the ringing of the probes. Thus a pulse-shaping circuit would be required for an eventual automatic device of this type for measuring cavitation mechanical intensity. For the moment we have preferred to postpone this approach in favor of a more "manual" one capable of providing much basic information on the actual signals obtained, and hence on the actual features of the bubble collapse, before launching into the design of a more automated MCA-type circuit. An alternative overall approach would be the development of microprobes of higher natural frequency, and this avenue may be pursued in the future. However, the final probe design must possess sufficient ruggedness to allow its application in various field conditions, so that eventual frequency response may be limited to the approximate range now obtained.

For the present study, pulse height spectra were developed by means of oscilloscope photographs and a threshold triggering circuit. Low frequency input, not of interest for cavitation bubble collapse, was suppressed by a high-pass filter set at frequencies $\leq$ 90 kHz. Very numerous scope photos were taken for each of the different system parameters investigated because of the very large variations in pulse counts at different amplitudes: 10^6-10^7/min. for low amplitudes vs. 10/min for large. From the viewpoint of cavitation damage it is of course only the large amplitude pulses which are of interest. This is confirmed by the already well known observation from high-speed motion-picture studies that only one in $\sim 10^4$-10^6 bubbles, appearing to collapse

near the surface, produces a visible crater even in soft materials (14,15, eg.). Simple numerical calculations based upon such previous motion pictures from our venturi (14, eg.) indicates that the number of bubbles traversing the venturi is such that on the average they should be well-separated, so that generally there should be little acoustic interference between different bubble collapses.

B. Experimental Results and Discussion (11)

1. Pulse Details

Figure 11 shows oscilloscope output from the Kistler and U-M probes for cavitation condition I and downstream pressure of 1 bar (gage) for $\sim$20°C water so that vapor pressure is negligible. Throat velocity for this condition (Table 1) is $\sim$12 m/s. It is assumed that each of the individual pulse groups are due to the collapse of single bubbles. In those cases where each probe registered approximately identical outputs, it is presumed that the bubble collapse occurred approximately equally distant from the two probes; i.e., not adjacent to either. This is the case for the first collapse in the upper right-hand photo. The second collapse seen by the Kistler in that case was apparently not seen by the U-M probe, thus presumably taking place close to the Kistler in that case. However, detailed examination of many such photos indicated no systematic difference between the two probe positions, thus confirming the essential axial-symmetry of the flow. Also as observed in the upper right-hand photo and elsewhere (Fig. 11), the first peak in each group is often not the highest. This may indicate that the registered amplitude is often severely truncated by the insufficiently fast response of the transducers. Further examination of Fig. 11 indicates the validity of the assumption that only single bubbles are in general active at a given time; hence the relatively large time-axis spacings between the pulse groups.

Figure 12 shows a direct comparison of the pulse count spectra generated from the Kistler and U-M probes exposed to the same cavitation field. While there is some slight difference between the spectra so formed, it is not great. In this particular case the U-M probe "sees" a somewhat greater number of collapses than does the Kistler.

2. Pulse Count Spectra

a. General

Figure 12 shows typical pulse count spectra generated from each probe in terms of "counts"/min. vs. peak pressure (psi). As already explained, the "counts" are the number of bubble collapses registered by the transducer. Pulse groups such as are shown in Fig. 11 are considered to correspond to a single collapse and thus form a single "count". Obviously some personal judgment is required for interpretation and some imprecision will result when the pulse count spectra are determined in this way. However, these are necessary disadvantages at this stage in the development of our technique.

Figure 13 compares pulse count spectra in terms of counts/min. vs. peak pressure (maximum observed amplitude from transducer output) for various of the conditions tested, investigating the effects of throat velocity (downstream tank pressure), extent of cavitating regime (cavitation conditions I or II - see Fig. 9), and gas content. The investigation of none of these effects is as yet complete. However, the preliminary results here presented show the interdependence of the pulse count spectra on all of these dependent parameters of this experiment.

b. Gas Content Effect

Gas (primarily air) content for these experiments, measured by conventional Van Slyke apparatus, was varied between a maximum of slightly more than saturation at STP (ie, $\sim$2.0 vol.%) to a fraction of that value

($\sim$ 0.6 %, saturation at STP, i.e. $\sim$ 1.2 vol.%). For most of the runs the lower gas content was used, producing the upper three curves in Fig. 13. High total gas content ($\sim$ 2.0 vol.%) somewhat in excess of saturation (STP), was used for the lower three runs depicted (Fig. 13). A direct comparison is possible between the upper condition II curve for 25 psig back-pressure, and the lower condition II curves for 1 bar and 5 bar. It is apparent that the number of counts producing any given peak pressure on the transducer was reduced by a factor $\sim 10^2$ for the higher air content runs. If it is assumed that the spectral areas (areas under N vs P curves) are roughly proportional to count number at a given peak pressure, and that damage rate is roughly proportional to spectral area (8,9,eg.), then damage rate (MDPR) would be reduced by $\sim 10^2$ by such a change in gas content. No definite conclusions of this type can yet be drawn from the present work, since no quantitative erosion measurements have as yet been made. However, it has long been known (15-17, eg.) that an increase of air content in this range does significantly reduce MDPR.

c. Throat Velocity and Downstream Pressure

Throat velocity increases with downstream pressure for a given cavitation condition (as shown in Table 1) in this venturi facility, and of course the expected strong increase of MDPR with velocity is well known (15-18, eg.). This effect is strongly illustrated also in Fig. 13 for the three high air content runs in the lower portion of the curve sheet. However, the effect is opposite for the two low air content runs at cavitation condition I in the upper portion of the curve. Again, since no quantitative damage data has been obtained in these tests, no final conclusions can be drawn. However, only a small velocity-damage effect was observed here in previous tests (14) with the same venturi geometry.

d. Cavitation Condition Effects

The effect of cavitation condition, i.e., extent of cavitating region (Fig. 9), for fixed downstream pressure, i.e., approximately fixed velocity (Table 1), is shown in Fig. 13, by comparing two of the upper curves (25 psig back-pressure). The pulse count at large peak transducer pressures (important for damage) are greater by $\sim$ 10 x for condition II. Thus the more fully developed cavitation condition II produces a higher pulse spectra than the cavitation condition closer to inception, i.e, I. This is partially because the probes are also located at position II (Fig. 9). Thus presumably less damage would be caused by condition I than by condition II to damage probes located at II. This result occurs in spite of the fact that the bubble collapsing pressure at the probe position (II) is greater for the less developed cavitation. Even though the cavitation region observed with the unaided eye in condition I does not extend to the probe position, presumably a sufficient number of large and energetic bubbles do penetrate that far. This conclusion is consistent with previous damage tests in this venturi (14,15, eg.).

e. Probe and Actual Surface Peak Pressure Amplitudes (11)

The peak pressure amplitudes seen by the microprobes (Fig. 13, eg. - see ref. 11 for full details and other examples) extend up to $\sim 10^2$ psi, obviously much too small to be damaging even to the 1100-0 aluminum specimens used. Yet considerable damage was obtained (Fig. 14) for many of the conditions tested in runs of only 15 min. duration. It is thus obvious that the measured pressure amplitudes are much smaller than those actually existing on the surface. In our opinion there are two major reasons for this discrepancy.

The first and most obvious is geometrical. The active area of the probes ($\sim$5 mm dia.) is much greater than the presumed microjet or shock-wave

diameter from a bubble collapsing on, and/or rebounding adjacent to, the damaged surface (19, eg.). In a previous study here by Kling (19, eg.) using 10^6 Hz motion pictures, the jet diameter appeared to be ~ 0.1 mm from an initial bubble diameter ~ 3 mm. Thus the jet (or impinging shock) area is probably $\sim 10^2$-10^4 that of the probe, giving a possible pressure multiplying factor of this order of magnitude, on geometrical accounts.

A second reason for the discrepancy between measured and actual surface pressures is the "inefficiency" of the probes themselves in recording possible nanosecond rise times (13, eg.), since probe natural frequencies are ~ 0.1 MHz. It is impossible to assign a definite value to the effect of the probe inefficiency, but we believe the factor could well be >10. Thus there may well be a total factor $\sim 10^3$-10^5 between measured and actual surface pressure magnitudes, so that peak surface pressures $\sim 10^5$-10^7 psi are indicated. Considerations such as damage to very hard materials make this range appear credible. Thus the present probes are not suitable for measuring actual surface bubble-collapse peak pressure amplitudes. However, the results should be at least roughly proportional to those measured and the pulse-count spectra can be used for damage prediction, once they are "calibrated" in an actual cavitation flow. This will be accomplished in the present study when actual MDPR and pit-count data become available, hopefully in the relatively near future.

3. Pulse Count Spectra and Erosion

Figure 15 shows the pulse count spectra developed for six different system conditions taken on the same day, using the same loop water, to avoid any variations on that account. At the same time, 1/4 in. (6.4 mm) diameter 1100-0 aluminum damage specimens were inserted flush with the wall at the same axial position as that of the microprobes (Fig. 9), and exposed to 15 min. of cavitation in each case, during which time the pressure pulse spectra

were generated. Thus in this condition there is one-to-one correspondence between the pulse spectra and the damage observed. Figure 16 is a schematic representation of the damage obtained, and Fig. 14 shows scanning electron microscope pictures of the damaged specimens. No exact pit counts or weigh loss measurements were made for these initial damage tests. However, it is apparent that significant damage was obtained only on specimens #4,5, and 6, and that these correspond to spectra showing appreciable numbers of counts in the higher peak pressure region. This is particularly true of #4 and 6, while #5 is somewhat more marginal. A close examination of #5 shows less damage than for #4 and 6. Thus at least a qualitative correlation between pulse count spectra and observed damage was obtained for these preliminary tests. More precise damage tests are planned for the near future.

IV. CONCLUSIONS

1. Cavitation damage tests in a vibratory facility in synthetic sea water and tap water, over a range of temperature and pressure conditions, with three materials of varying degrees of corrodibility, indicate that the ratio between maximum MDPRs for salt and fresh water tests increases toward unity as the "mechanical" cavitation intensity is increased, either by increasing suppression pressure or varying liquid temperature toward the maximum damage condition. This result is expected on theoretical grounds.

2. The expected trend of increased incubation period for reduced maximum MDPR is verified for these vibratory facility tests for all the materials considered togethered, ie., 304-SS, 1018 carbon steel, and 1100-0 aluminum. However, it is clear that precise nature of the relationship between incubation period and maximum MDPR depends on the properties of the materials themselves.

3. A technique involving pulse height spectra from submerged pressure microprobes has been developed and used in a cavitating water venturi to measure cavitation bubble collapse "mechanical" intensity, and to correlate

this parameter with observed erosion. Only a qualitative correlation has yet been obtained in the venturi, although more precise correlations were previously obtained here using a more preliminary version of the same system in our vibratory facility (8,9).

4. Pulse height spectra have been used in the present study to measure the effect upon "mechanical" cavitation intensity of various parameters such as total gas content, throat velocity, and cavitation condition (extent of cavitating region). The results are reasonably consistent with previous expectations in these regards.

5. The microprobes used (one developed here for high temperature use and one commercial) are suitable for the purpose of providing a practical means of measuring mechanical cavitation intensity, and thus providing an à priori prediction of eventual erosion rates, pertinent to various flowing laboratory and field devices. The resultant pulse height spectra can be used to measure a "cavitation erosion efficiency" which compares acoustic power delivered to an eroded surface with erosion power, defined as the product of material ultimate resilience and volume loss rate (8,9).

6. The microprobes used are not capable of following in detail the pressure pulsations resulting from bubble collapse in a cavitating field , due to insufficient time response rate. However, for probes of practical utility and adequate ruggedness, it may not be possible to improve this situation greatly. The present probes appear adequate for the purpose of damage prediction.

V. ACKNOWLEDGMENTS

The work here reported was supported by the Office of Naval Research Contract No. N00014-76-C-0697. Mr. Stanley W. Doroff was project monitor.

REFERENCES

1. I. S. Pearsall, P. J. McNulty, "Comparisons of Cavitation Noise with Erosion," 1968 ASME Cavitation Forum, p. 6-7.

2. W. M. Deeprose, N. W. King, P. J. McNulty, I. S. Pearsall, "Cavitation Noise, Flow Noise and Erosion," Proc. Conf. on Cavitation, Inst. Mech. Engrs., Fluid Machinery Group, Herriot-Watt Univ., Edinburgh, Sept. 1974, 373-381.

3. J. J. Varga, Gy. Sebestyen, "Determination of Hydrodynamic Cavitation Intensity by Noise Measurement," Proc. 2nd International JSME Symp. on Fluid Machinery and Fluidics, Tokyo, Sept. 1972, 285-292.

4. J. J. Varga, Gy. Sebestyen, A. Fay, "Detection of Cavitation by Acoustic and Vibration-Measurement Methods," La Houille Blanche, 2, 1969, 137-149.

5. F. Numachi, "Transitional Phenomena in Ultrasonic Shock Waves Emitted by Cavitation on Hydrofoils," Trans. ASME, J. Basic Engr., 81, June 1959, p.153.

6. F. Numachi, "An Experimental Study of Accelerated Cavitation Induced by Ultrasonics," Trans. ASME, J. Basic Engr., 87, 1965, 967-976.

7. V. K. Mukarov, A. A. Kortnev, S. G. Suprun, G. I. Okolelov, "Cavitation Erosion Spectra Analysis of Pulse-Heights Produced by Cavitation Bubbles," Proc. 6th Non-Linear Acoustics Conference, Moscow, July 1975.

8. F. G. Hammitt, S. A. Barber, M. K. De, An. N. El Hasrouni, "Predictive Capability for Cavitation Damage from Bubble Collapse Pulse Count Spectra," Proc. Conf. on Scaling for Performance Prediction in Rotodynamic Machines, Inst. Mech. Engrs., Sept. 6-8, 1977, Univ. of Stirling, U.K.

9. F. G. Hammitt, S. A. Barber, M. K. De, A. N. El Hasrouni, "Cavitation Damage Prediction from Bubble Collapse Pulse Count Spectra," 1977 ASME Cavitation and Polyphase Flow Forum, June 1977, 25-28.

10. F.G. Hammitt, Ph. N. Hasrouni, A. N. El Hasrouni, G. Vaghidas, "Vibratory Facility Cavitation Damage Tests: Tap Water vs. Synthetic Sea Water," ORA Report No. UMICH 014456-18-I, May 1977, Univ. of Mi., Ann Arbor, Mich.

11. M. K. De, "Emission and Transport of Shock Waves from Pulsating Cavities in High Speed Fluid Flow and Their Incidence on a Solid Surface," ORA Report No. UMICH 014456-22-I, July , 1977, Univ. of Mich., Ann Arbor, Mich.

12. F. G. Hammitt, "Cavitation Damage and Performance Research Facilities," ASME Symp. on Cavitation Research Facilities and Techniques, 1964, 175-184

13. W. Lauterborn, K. J. Ebeling, "High-Speed Holography of Laser-Induced Cavitation Bubbles in Liquids," Proc. of 7th International Symp. on Nonlinear Acoustics, Aug. 19-21, 1976, Blacksburg, Va.

14. M. J. Robinson, F. G. Hammitt, "Detailed Damage Characteristics in a Cavitating Venturi," Trans. ASME, J. Basic Engr., 89, D, 1, Mar. 1967, 161-173.

15. R. T. Knapp, J. W. Daily, F. G. Hammitt, Cavitation, McGraw-Hill, 1970.

16. R. E. H. Rasmussen, "Some Experiments on Cavitation Erosion in Water Mixed with Air," Proc. 1955 NPL Symp. on Cavitation in Hydrodynamics, Paper 20, HMSO, London, 1956.

17. J. M. Mousson, "Pitting Resistance of Metals Under Cavitation Conditions," Trans. ASME, 59, 1937, 399-408.

18. R. T. Knapp, "Recent Investigations of Cavitation and Cavitation Damage," Trans. ASME, 77, 1955, 1045-1054.

19. C. L. Kling, F. G. Hammitt, "A Photographic Study of Spark-Induced Cavitation Bubble Collapse," Trans. ASME, J. Basic Engr., 94, D, 4, Dec. 1972, 825-833.

List of Figures

Table 1

Summary of Venturi Test Parameters

P_{out} (psig)	V_I (m/s)	V_{II} (m/s)
0	11.6	14.7
10	13.7	16.8
25	18.9	22.9
50	28.9	36.6

Notes:

P_{out} = outlet pressure from venturi

V_I = venturi throat velocity at cavitation condition - I

V_{II} = venturi throat velocity at cavitation condition - II

1 ATM = 14.7 psi

Fig. 1 Correlation of Pulse Pressure Spectrum Area and MDPR

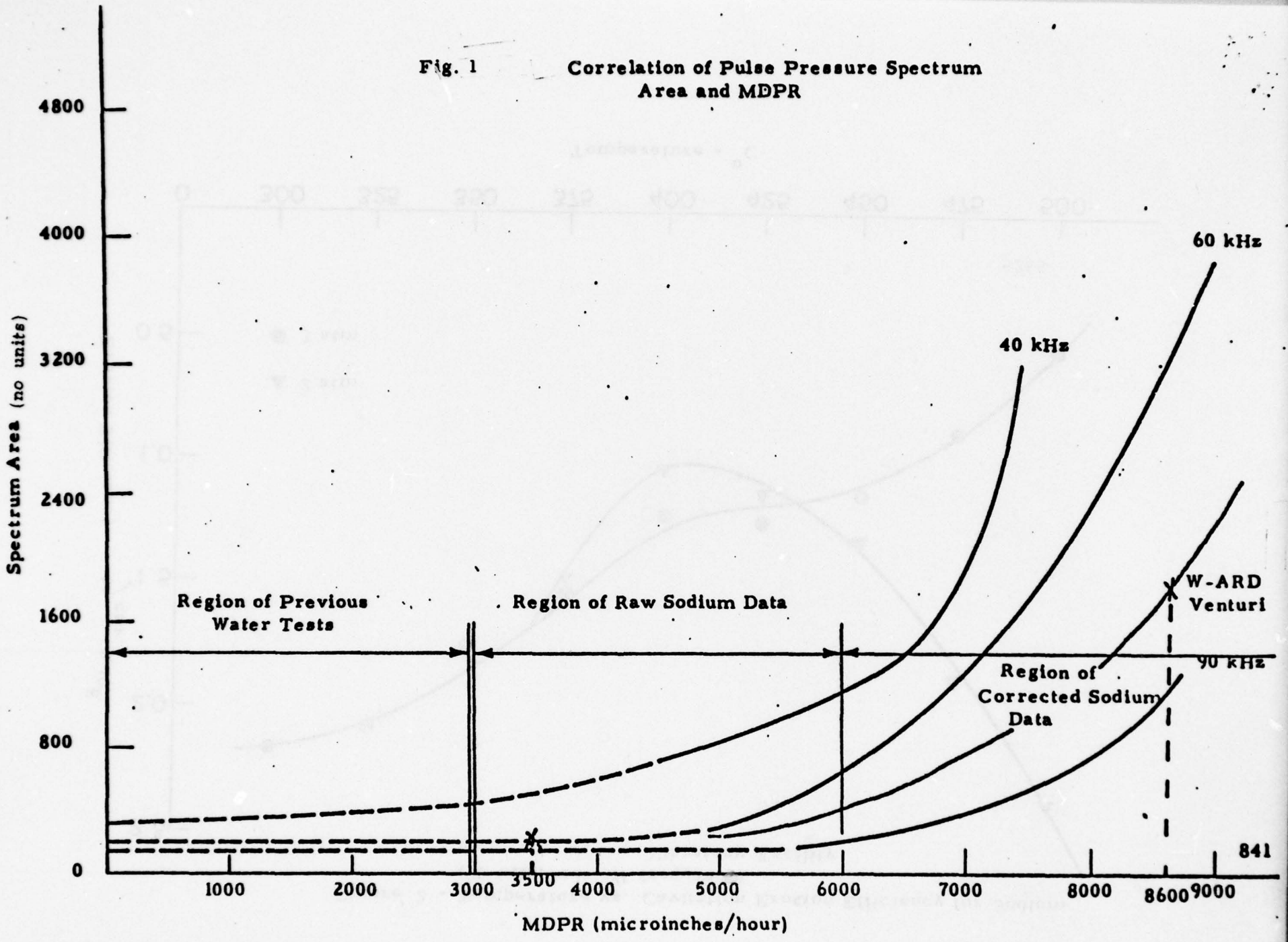

Figure 2 - Temperature vs. Cavitation Erosion Efficiency for Sodium
(70 kHz. cut-off frequency)
Vibratory Facility

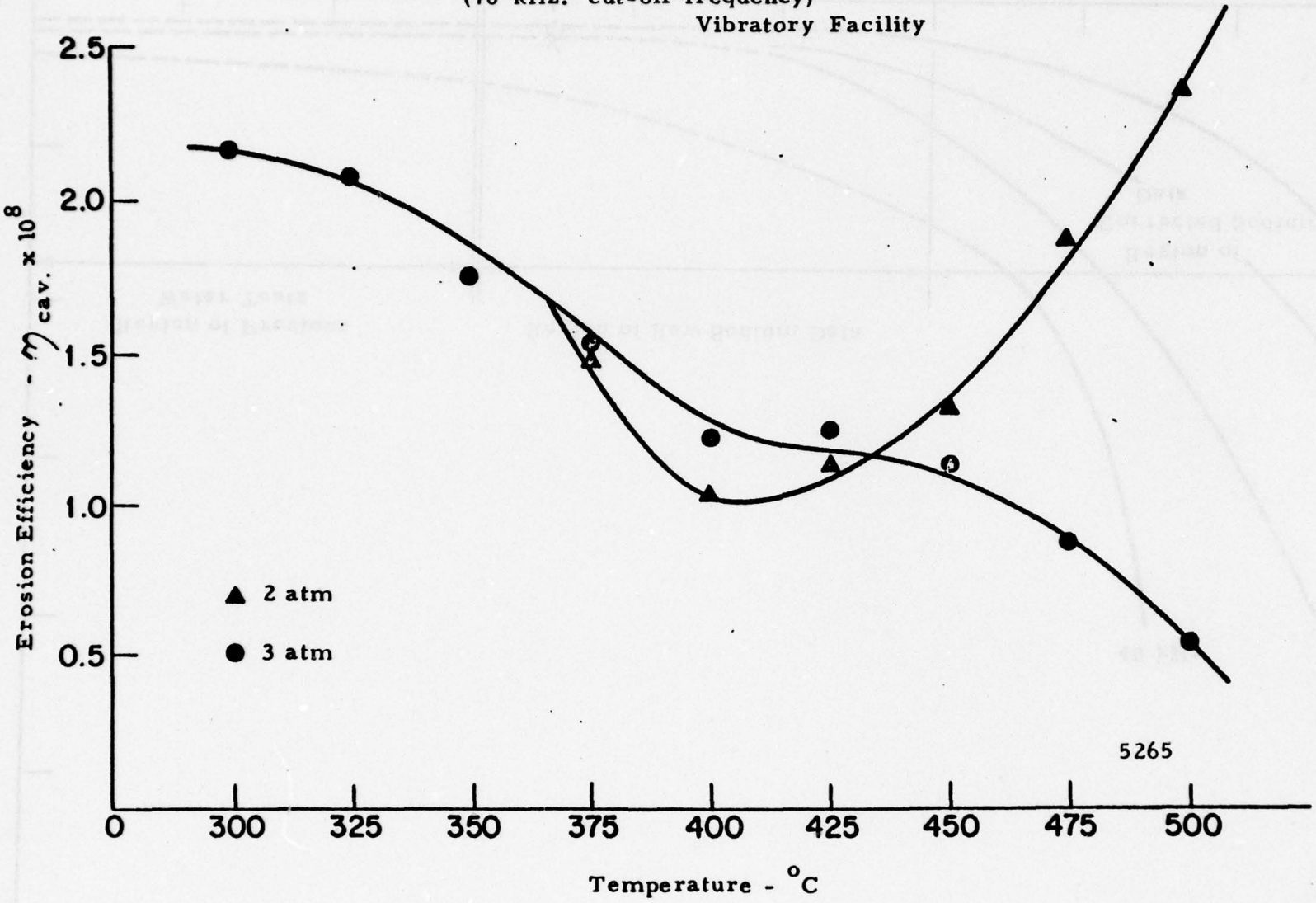

Fig. 3. Ratio of Maximum MDPR(s), Fresh/Salt Water vs. Maximum MDPR(s) for Fresh Water (SS-304)

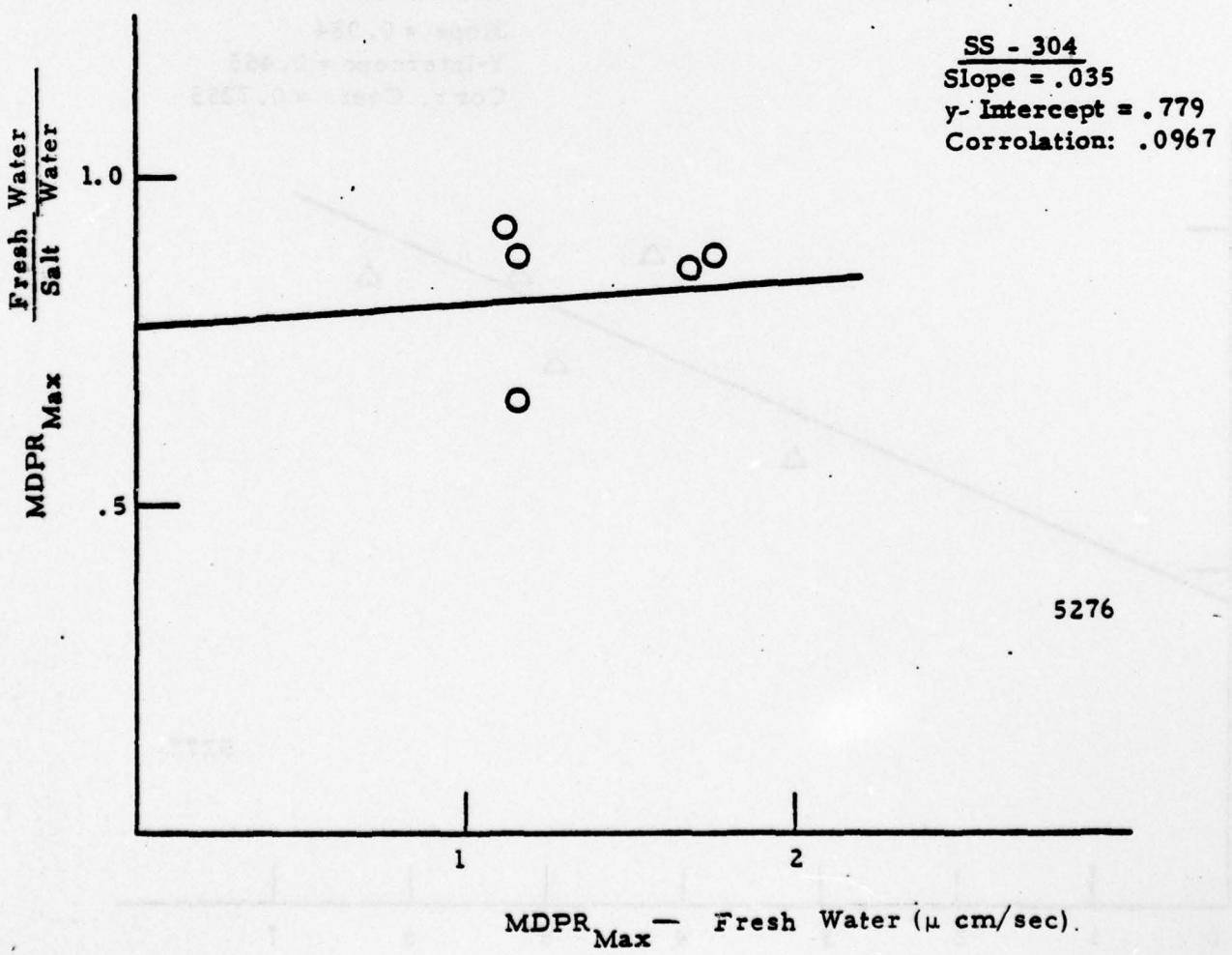

Fig. 4 - Ratio of Maximum MDPR(s), Fresh/Salt Water vs. Maximum MDPR(s) for Fresh Water (C/S-1018)

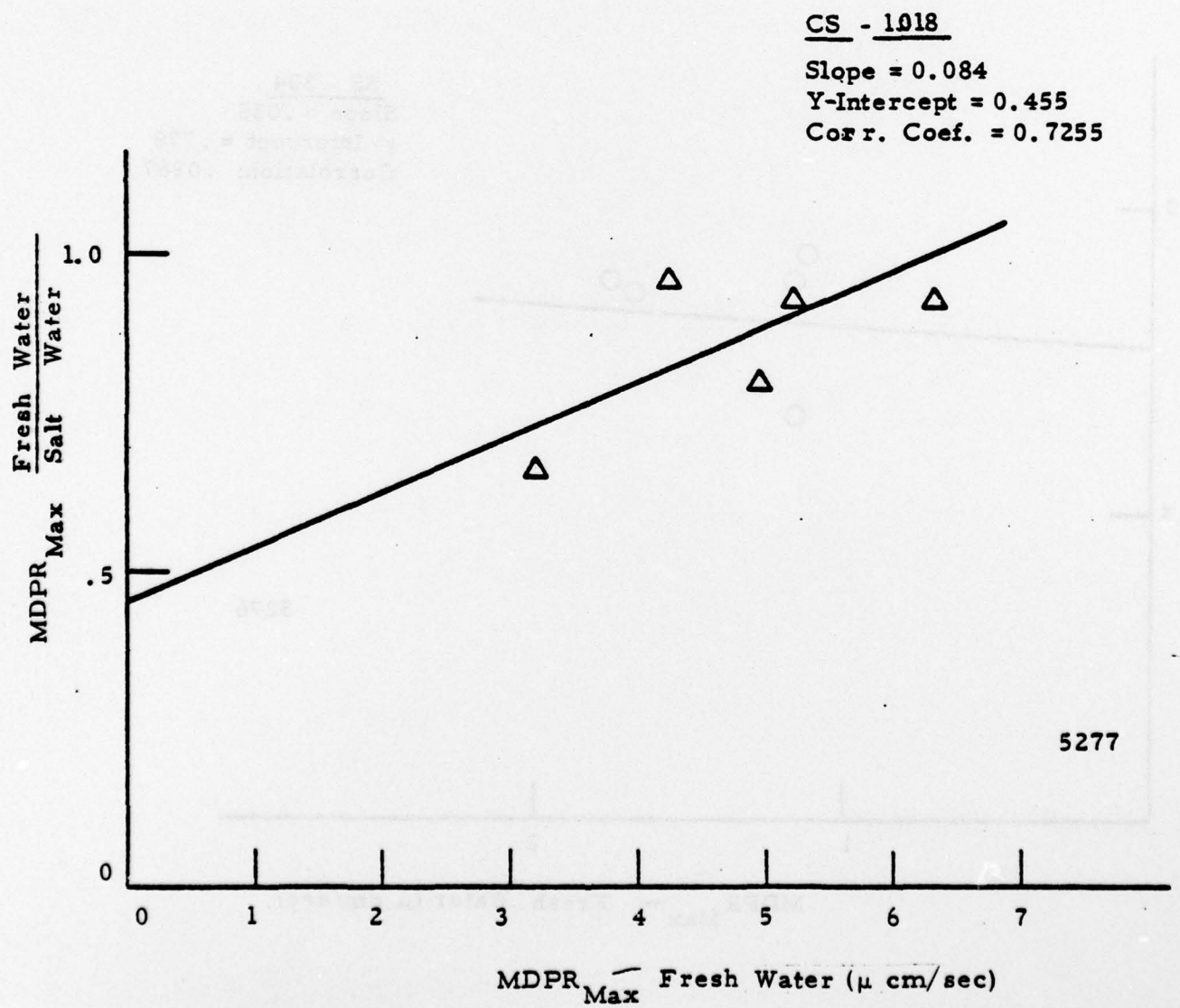

Fig. 5 -Incubation Period vs. Maximum MDPR for SS-304

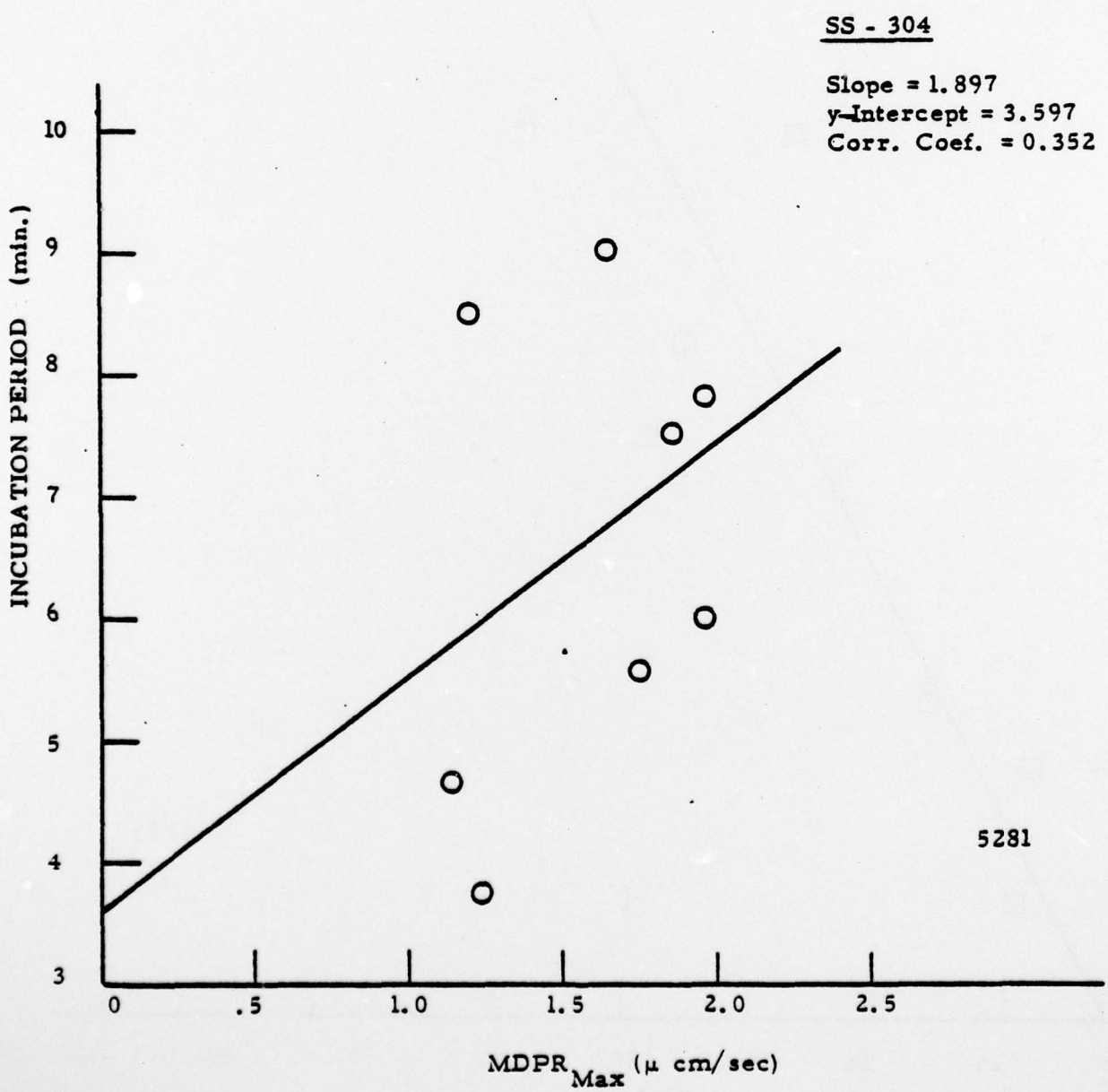

Fig. 6 - Incubation Period vs. Maximum MDPR for 1100-0 Alum. in Vibratory Facility

slope = .0462
y-intercept = -0.519
corr. Coef. = 0.883

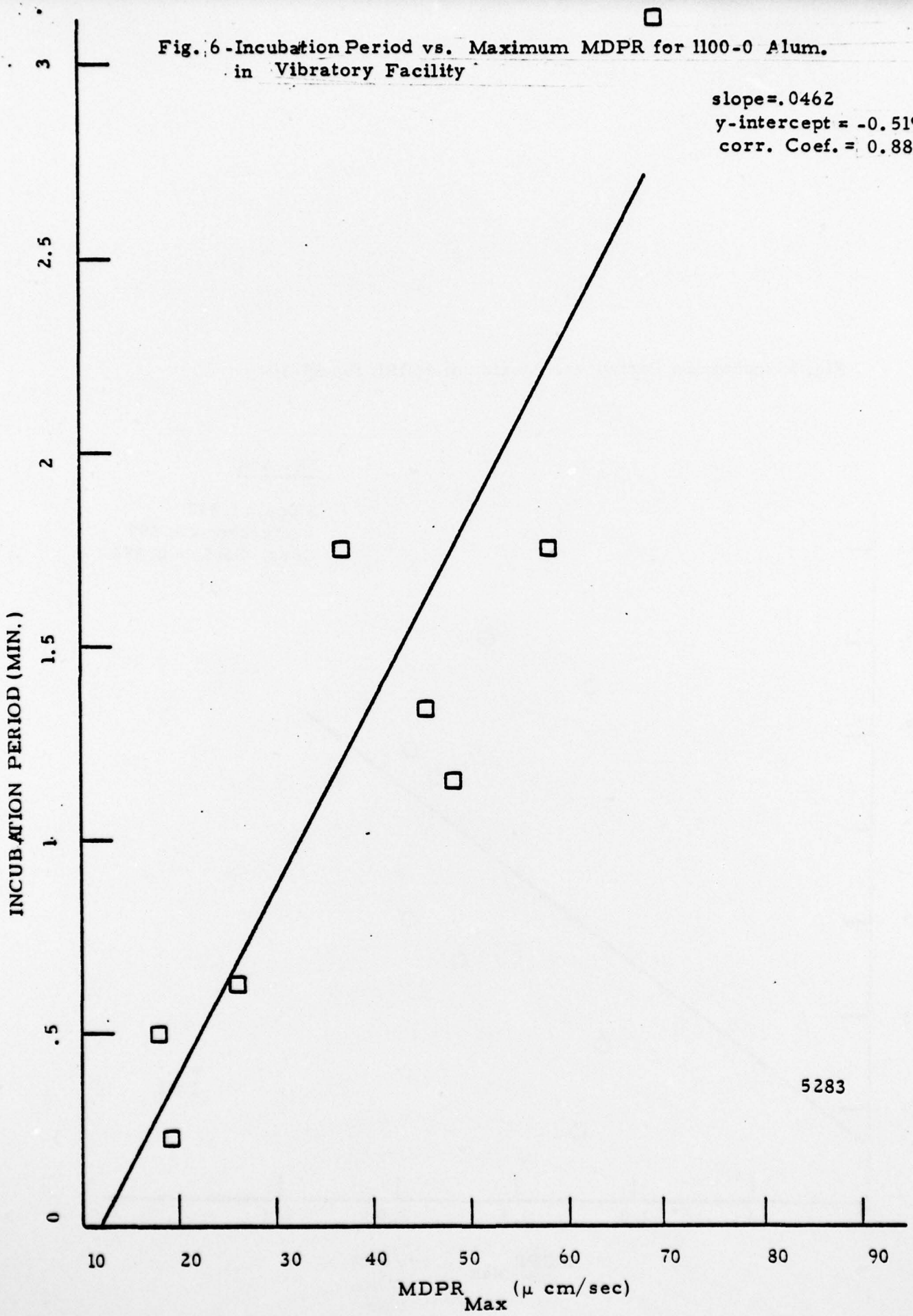

Fig. 7 - Incubation Period vs. Maximum MDPR for all Materials in Vibratory Facility

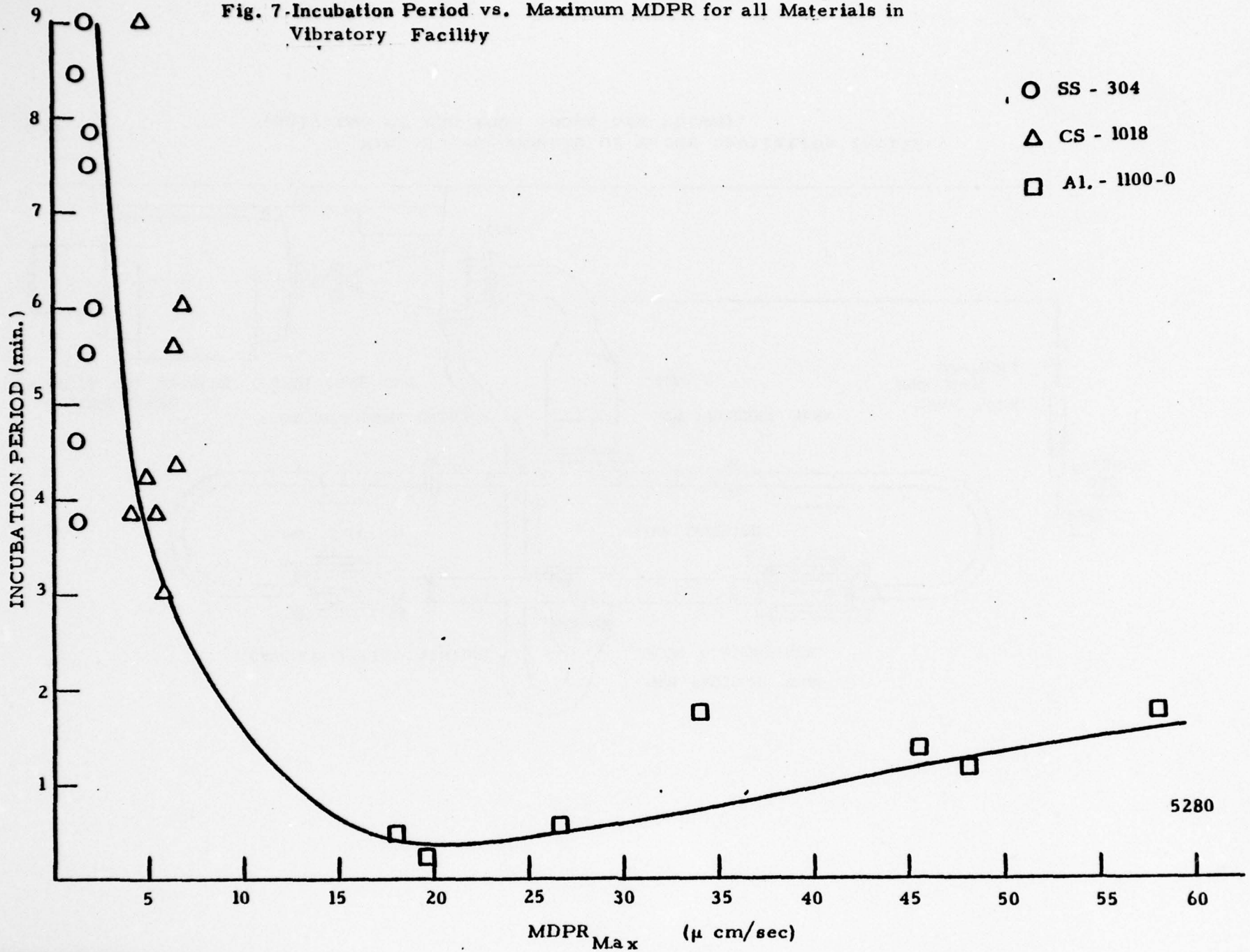

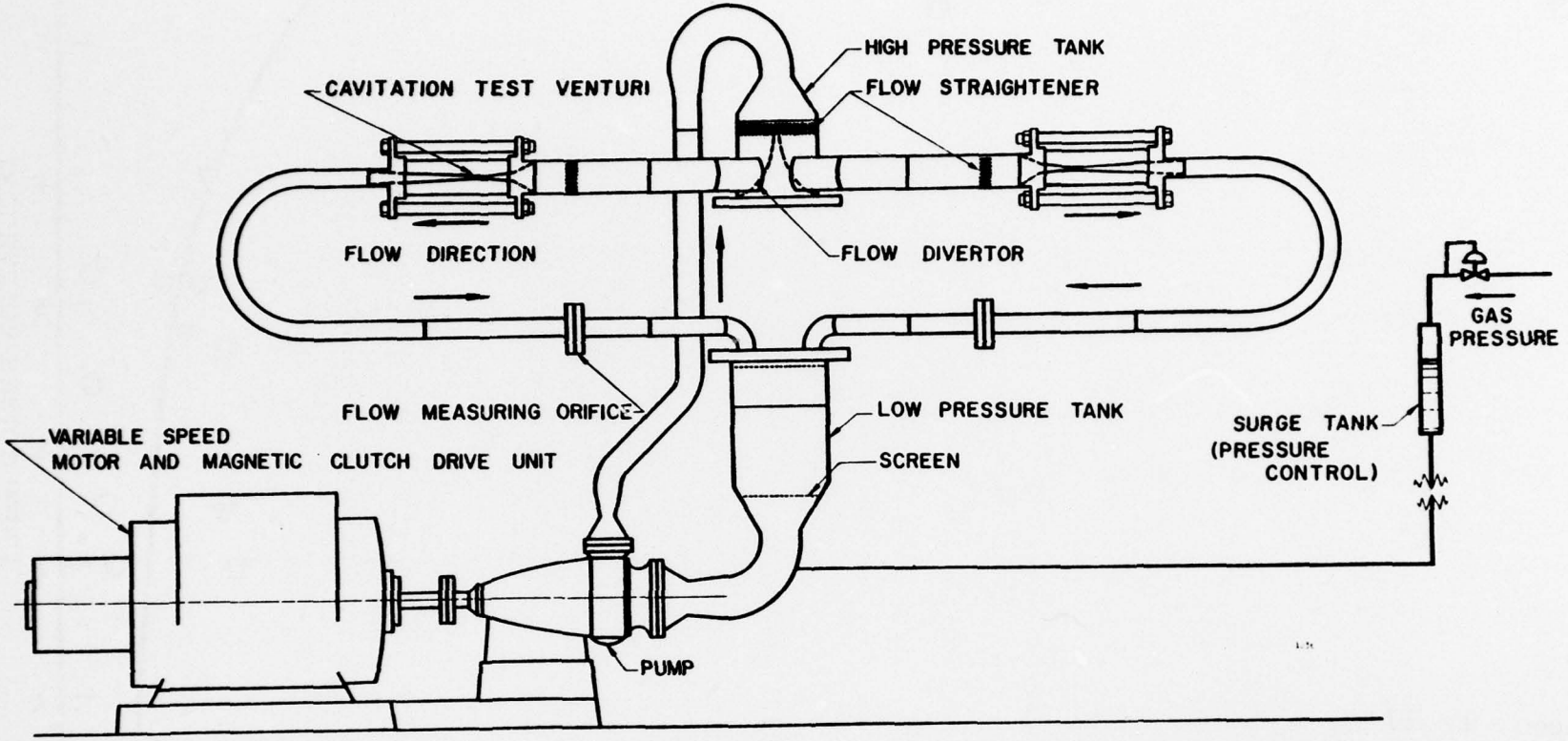

Fig. 8.--Schematic of water cavitation facility (only two of the four loops are shown).

Cylindrical Venturi

FIG 9

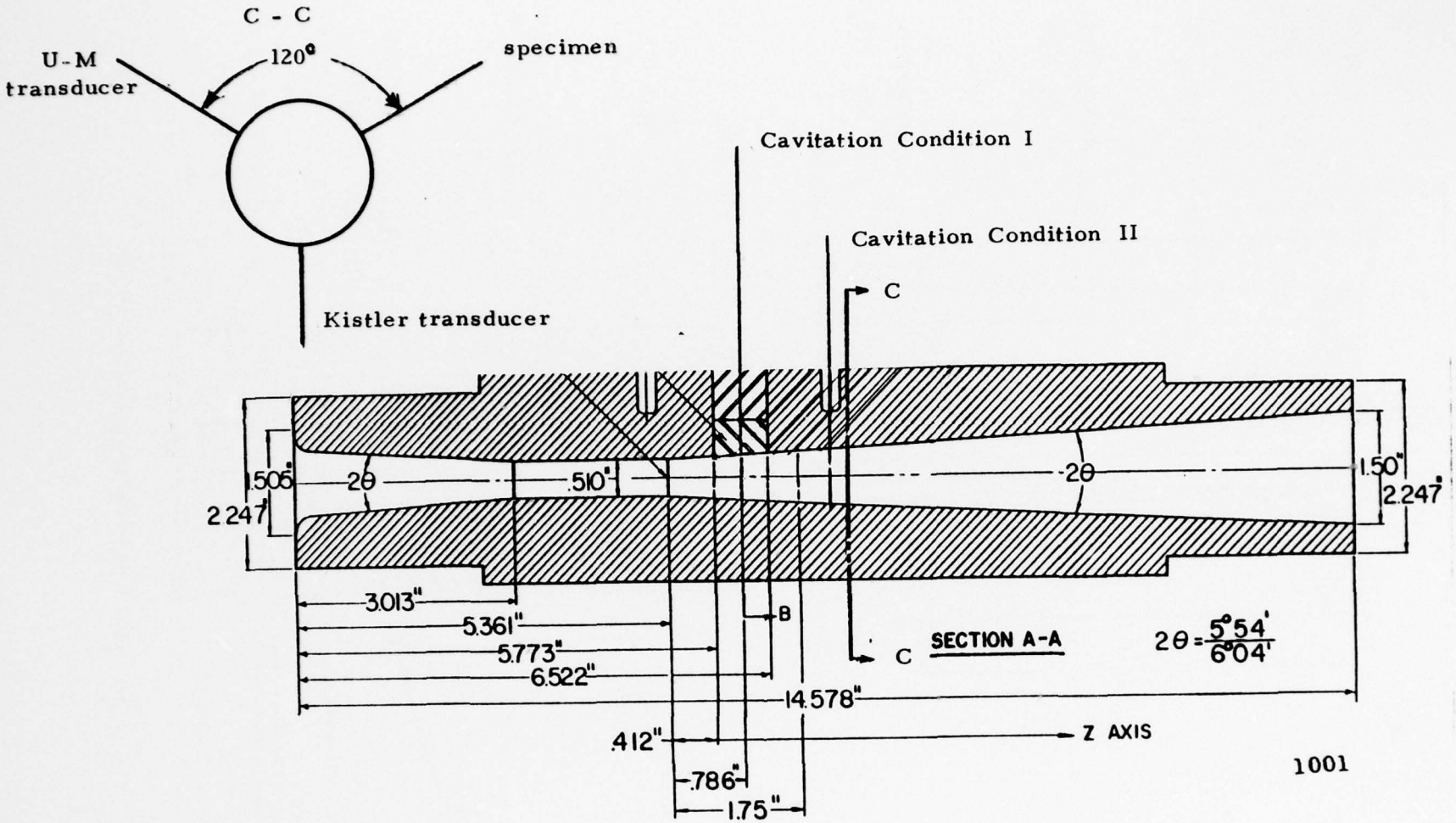

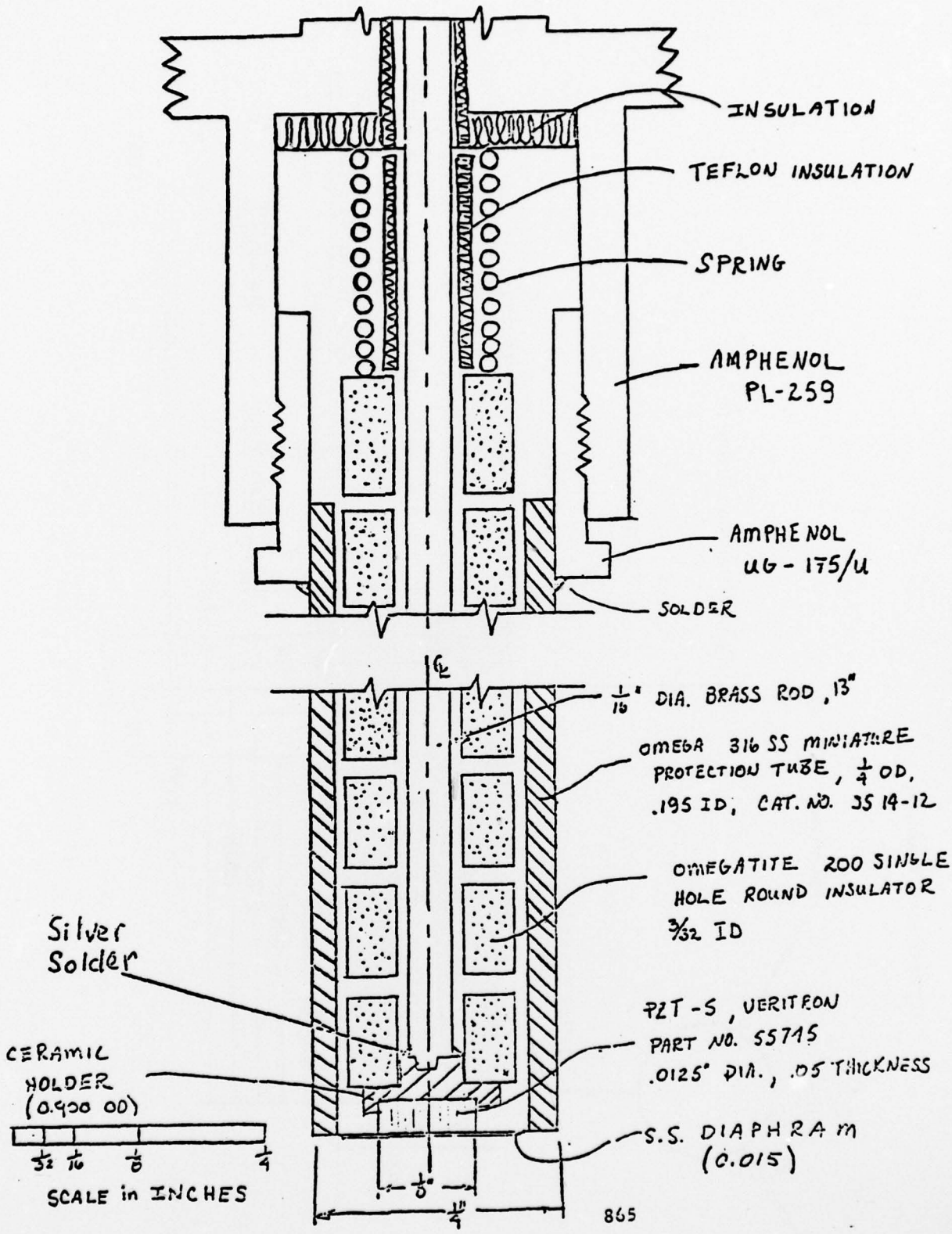

U-M High Temperature Acoustic Probe

FIG 10

Response of U-M and Kistler Microprobes (positioned on a plane of Symmetry in a Venturi) to pressure waves emanated by Collapsing Cavities.

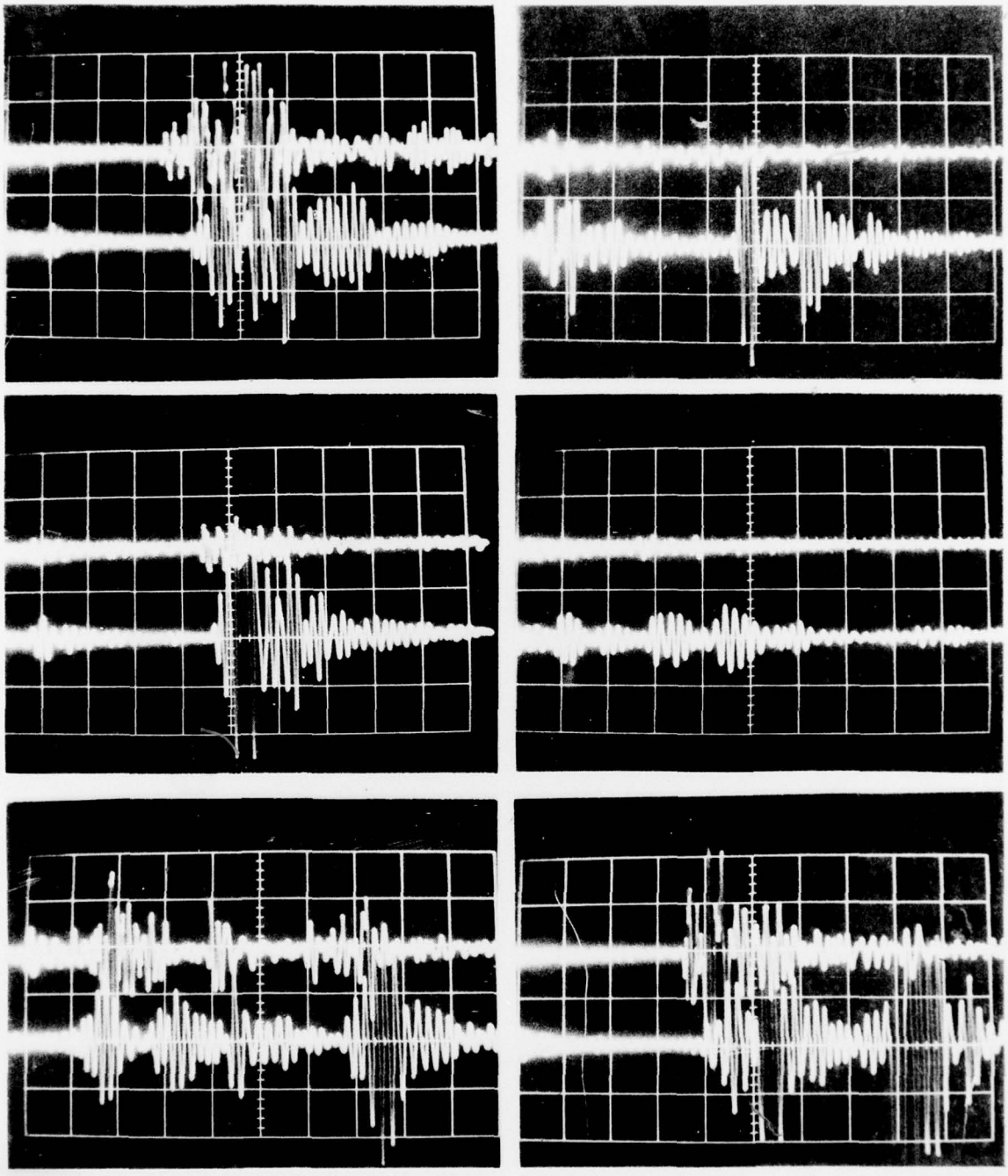

Fig. 11

Fig. 12 Comparison of U-M and Kistler Microprobes
Integral Distribution of Pressure Pulses

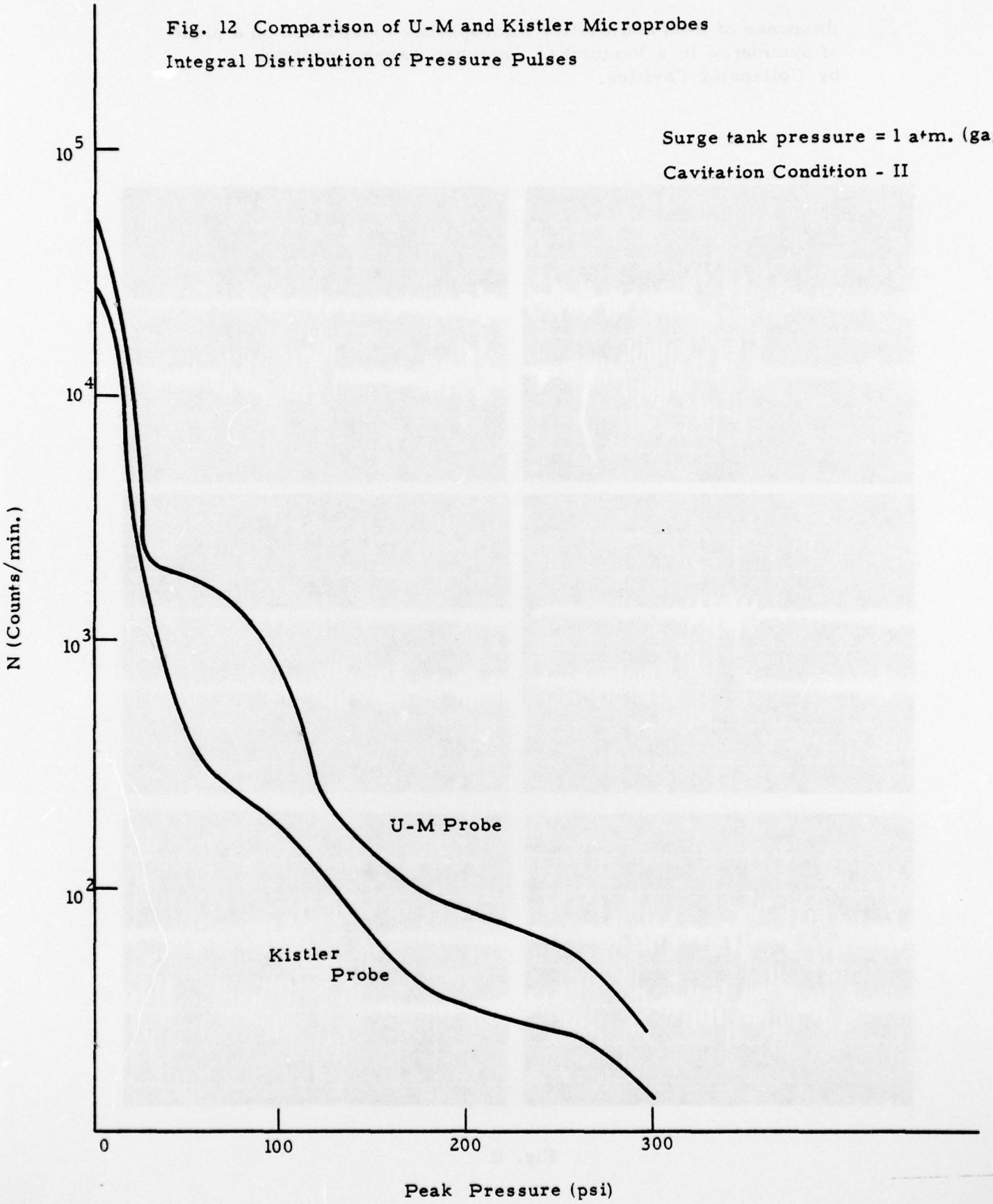

FIG 13

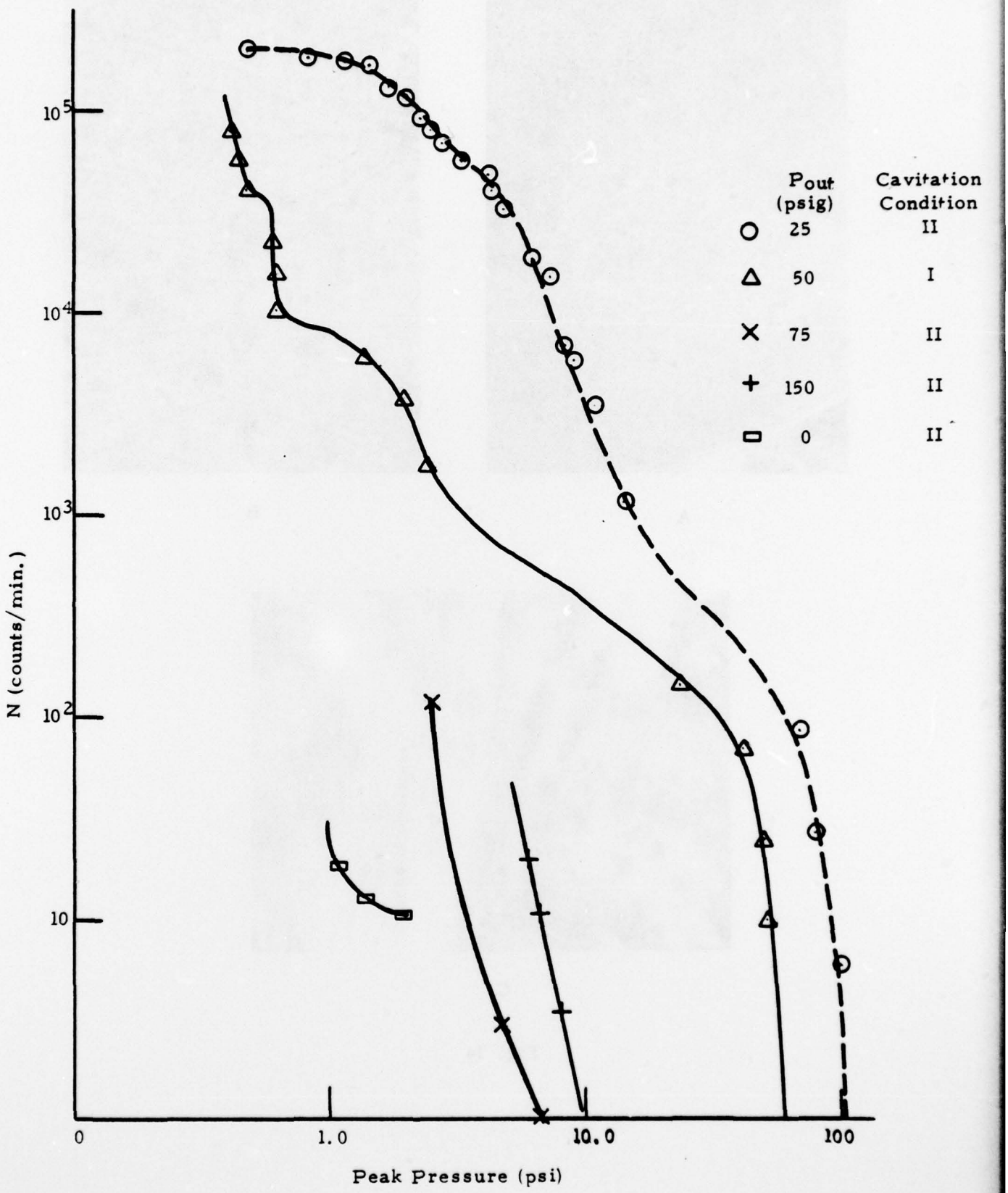
10^5
10^4
10^3
10^2
10
N (counts/min.)
0
1.0
10.0
100
Peak Pressure (psi)
Pout (psig)
Cavitation Condition
25
II
50
I
75
II
150
II
0
II

A

B

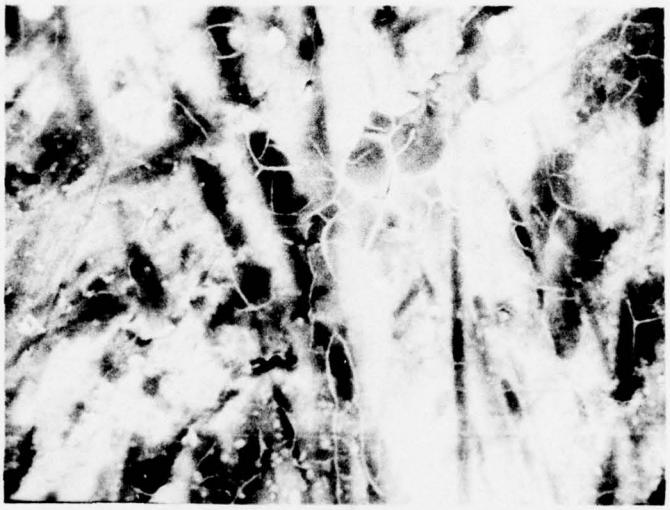

C

Fig. 14

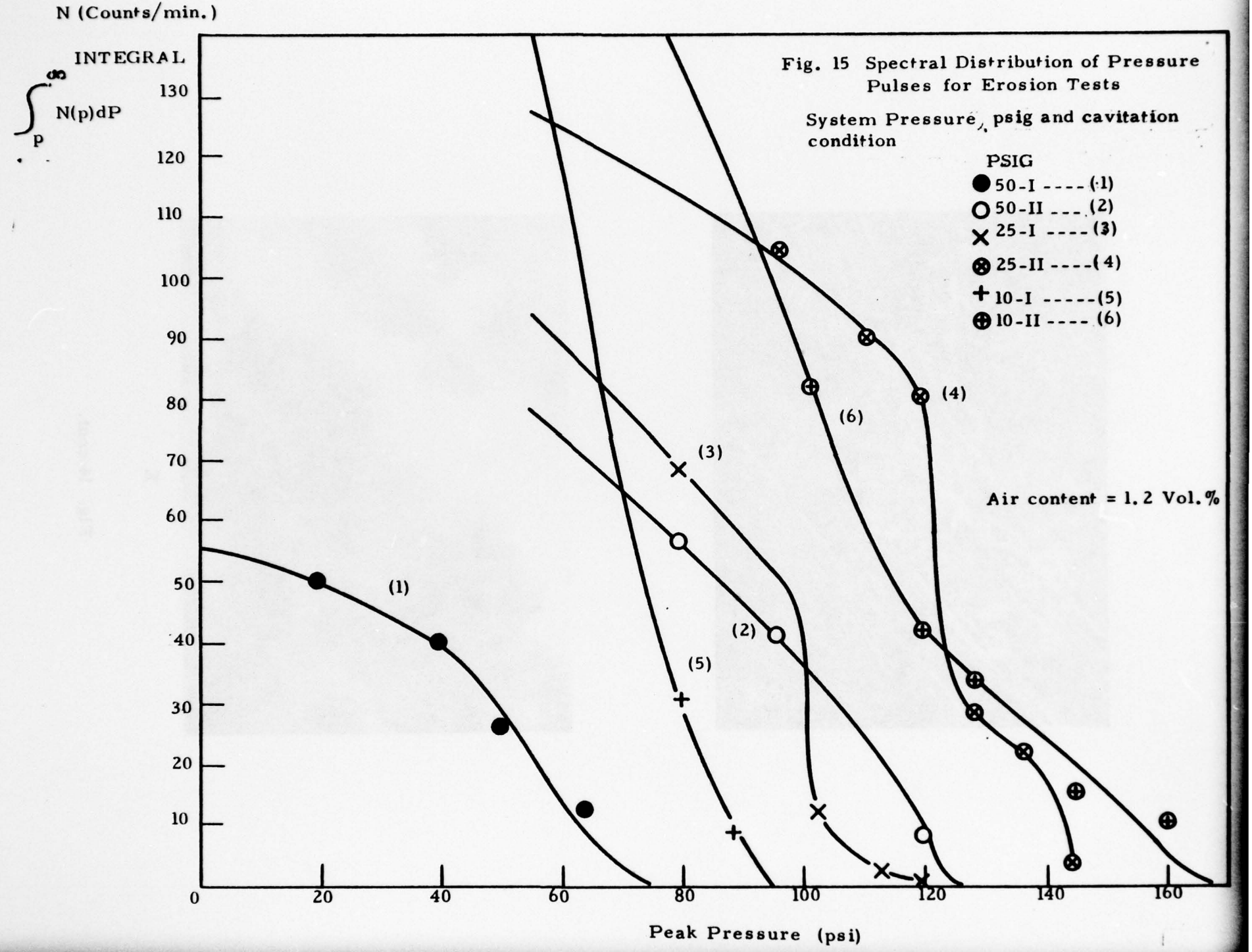
N (Counts/min.)
INTEGRAL
$\int_p^{\infty} N(p)dP$
130
120
110
100
90
80
70
60
50
40
30
20
10
0
20
40
60
80
100
120
140
160
Peak Pressure (psi)
Fig. 15 Spectral Distribution of Pressure Pulses for Erosion Tests
System Pressure, psig and cavitation condition
PSIG
50-I ---- (1)
50-II --- (2)
25-I ---- (3)
25-II ---- (4)
10-I ----- (5)
10-II ---- (6)
Air content = 1.2 Vol.%
(1)
(2)
(3)
(4)
(5)
(6)

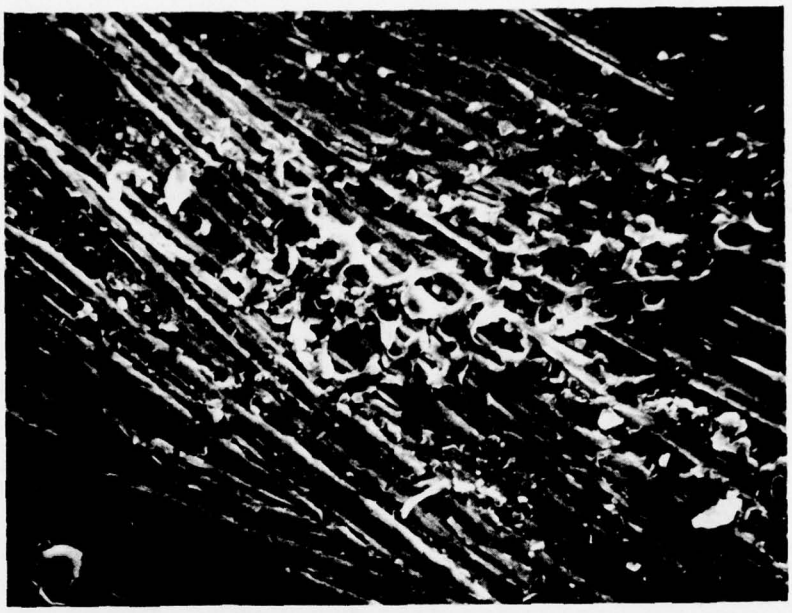

D

E

Fig. 14 cont.

1100 - 0 Aluminum Specimens after exposure to Shock Waves

FIG 16